Biogeosciences Discuss., 9, 8571–8610, 2012
www.biogeosciences-discuss.net/9/8571/2012/
doi:10.5194/bgd-9-8571-2012

Biogeosciences Discussions

A ^{13}C labelling study on carbon fluxes in Arctic plankton communities under elevated CO_2 levels

A. de Kluijver[1], K. Soetaert[1], J. Czerny[2], K. G. Schulz[2], T. Boxhammer[2], U. Riebesell[2], and J. J. Middelburg[1,3]

[1]Department of Ecosystems Studies, Royal Netherlands Institute for Sea Research (NIOZ) (formerly: Netherlands Institute of Ecology, NIOO-KNAW), Yerseke, The Netherlands
[2]Helmholtz Centre for Ocean Research Kiel (GEOMAR), Kiel, Germany
[3]Faculty of Geosciences, Utrecht University, Utrecht, The Netherlands

Received: 7 June 2012 – Accepted: 11 June 2012 – Published: 17 July 2012

Correspondence to: A. de Kluijver (anna.de.kluijver@nioz.nl)

Published by Copernicus Publications on behalf of the European Geosciences Union.

Abstract

The effect of CO_2 on carbon fluxes in Arctic plankton communities was investigated during the 2010 EPOCA mesocosm study in Ny Ålesund, Svalbard. Nine mesocosms were set up with initial pCO_2 levels ranging from 185 to 1420 µatm for 5 weeks. ^{13}C labelled bicarbonate was added at the start of the experiment to follow the transfer of carbon from dissolved inorganic carbon (DIC) into phytoplankton, bacteria, total particulate organic carbon (POC), zooplankton, and settling particles. Polar lipid derived fatty acids (PLFA) were used to trace carbon dynamics of phytoplankton and bacteria and allowed distinction of two groups of phytoplankton: phyto I (autotrophs) and phyto II (mixotrophs). Nutrients were added on day 13. A nutrient-phytoplankton-zooplankton-detritus model amended with ^{13}C dynamics was constructed and fitted to the data to quantify uptake rates and carbon fluxes in the plankton community during the phase prior to nutrient addition (phase 1, days 0–12).

During the first 12 days, a phytoplankton bloom developed that was characterized by high growth rates (0.87 $days^{-1}$) for phyto I and lower growth rates (0.18 $days^{-1}$) for phyto II. A large part of the carbon fixed by phytoplankton (~31 %) was transferred to bacteria, while mesozooplankton grazed only ~6 % of the production. After 6 days, the bloom collapsed and part of the organic matter subsequently settled into the sediment traps. The sedimentation losses of detritus in phase 1 were low (0.008 $days^{-1}$) and overall export was only ~7 % of production. Zooplankton grazing and detritus sinking losses prior to nutrient addition were sensitive to CO_2: grazing decreased with increasing CO_2, while sinking increased.

Phytoplankton production increased again after nutrient addition on day 13. Although phyto II showed initially higher growth rates with increasing CO_2 (days 14–22), the overall production of POC after nutrient addition (phase 2, days 14–29) decreased with increasing CO_2. Significant sedimentation occurred towards the end of the experiment (after day 24) and much more material settled down in the sediment traps at low CO_2.

BGD
9, 8571–8610, 2012

1 Introduction

About 30 % of anthropogenic CO_2 has accumulated in the oceans causing modification of the oceans' chemistry. The most important impacts of anthropogenic CO_2 on marine carbonate chemistry are higher concentrations of CO_2 and a concurrent drop in pH, collectively referred to as ocean acidification. The CO_2 uptake capacity of the oceans is influenced by the plankton organisms that live in the surface waters. The flux of CO_2 from atmosphere to oceans is largely controlled by three biological processes: primary production, community respiration, and export (biological pump). Primary production and subsequent sinking of organic matter (OM) to depth increases the ocean's uptake capacity for CO_2. Community respiration in the upper ocean, dominated by heterotrophic bacteria, converts organic carbon back into CO_2 and thus decreases the ocean's CO_2 uptake capacity (Rivkin and Legendre, 2001). Understanding the effects of increasing CO_2 levels on these three processes is central to predict the ocean's response to rising atmospheric pCO_2. Particularly production and export showed to be potentially sensitive to changes in CO_2 (Riebesell et al., 2009).

The high-latitude oceans are especially vulnerable for anthropogenic CO_2 disturbances, because of lower temperatures. The solubility of CO_2 increases with decreasing temperatures, so that polar oceans contain naturally high CO_2 and low carbonate ion concentrations. With a lower buffer capacity, pH changes are considerably larger in the polar regions than at lower latitudes for future climate scenarios (Steinacher et al., 2009). Our knowledge about the potential effects of ocean acidification on plankton communities in polar regions is limited, but plankton community studies have been done in mid-latitude regions. In a mesocosm experiment in a Norwegian Fjord (Bergen in 2005) an increased inorganic carbon consumption relative to nutrient (N,P) uptake was observed at higher CO_2 levels in natural plankton communities (Riebesell et al., 2007; Bellerby et al., 2008). The enhanced uptake was not reflected in increased organic matter production (Schulz et al., 2008; de Kluijver et al., 2010) nor in increased bacterial activity (Algaier et al., 2008; de Kluijver et al., 2010) so enhanced export

BGD
9, 8571–8610, 2012

was the suggested sink for the extra carbon consumed at elevated pCO_2 (Riebesell et al., 2007). A proposed mechanism is that CO_2 induced carbon overconsumption is exuded by phytoplankton as dissolved organic matter (DOM), which aggregates with other particles and increases export (Engel et al., 2004a). In another mesocosm experiment (Bergen 2001) no CO_2 effects on primary production (DeLille et al., 2005) were recorded, but a stimulating effect of CO_2 on bacterial activity was observed (Engel et al., 2004b; Grossart et al., 2006). In the mesocosm studies mentioned above, nutrients were added to stimulate phytoplankton production at the start of the experiments, so CO_2 effects on a eutrophic, blooming community were observed. However, throughout most of the year, plankton communities exist under low nutrient conditions dominated by regenerated production, rather than new production (Legendre and Rassoulzadegan, 1995).

This mesocosm study is the first to investigate the effects of elevated CO_2 on high-latitude plankton communities and on plankton communities in a post-bloom, nutrient regenerating state. In summer 2010, nine mesocosms were set up in Kongsfjorden, Svalbard, with a range of CO_2 levels and monitored for changes in plankton community functioning. To study the uptake of carbon by phytoplankton (primary production) and subsequent transfer to bacteria and zooplankton (community respiration) and settling material (export), ^{13}C-DIC was added as a tracer. The ^{13}C labelling dynamics of phytoplankton and bacteria were determined by compound-specific isotope analyses of fatty acid biomarkers. This technique has been successfully applied in the previous CO_2 enrichment mesocosm experiment (in Bergen, year 2005) to study the interactions between phytoplankton and bacteria (de Kluijver et al., 2010). In addition to the previous mesocosm experiment (Bergen, 2005), ^{13}C POC and zooplankton analyses as well as quantitative sediment traps samples were included in this mesocosm study. A nutrient-phytoplankton-zooplankton-detritus model was constructed to quantify uptake and loss parameters and carbon flows in the mesocosms. The obtained parameters and fluxes were tested for CO_2 sensitivity.

BGD
9, 8571–8610, 2012

2 Materials and methods

2.1 Experimental setup and sampling

The mesocosm experiment was carried out in Kongsfjorden, Svalbard (78° 56.2′ N; 11° 53.6′ E) in June–July 2010 as part of the 2010 EPOCA (European project on Ocean Acidification) Arctic campaign. The experimental setup and mesocosm characteristics are described in detail in (Czerny et al., 2012). Briefly, 9 mesocosms of ~50 m^3 were deployed in the Kongsfjorden, about a mile off Ny Ålesund, on 28 May 2010. During lowering to ~15 m depth, the bags filled with nutrient-poor, post-bloom fjord water. A 3 mm mesh size net was used to exclude large organisms. The bags were closed on 31 May 2010, defined as time t_{-7} and time steps (t) continued per day. The CO_2 manipulation was done in steps over 5 days, from t_{-1} to t_4 by adding calculated amounts of CO_2 enriched seawater to each mesocosm. The main additions were done from t_{-1} to t_2 and a final adjustment was done on t_4. A range of initial pCO_2 levels of ~185–1420 µatm was achieved (exact CO_2 levels are provided in Bellerby et al., 2012). Due to gas exchange and photoautotrophic uptake pCO_2 levels declined in the mesocosms, especially in the high CO_2 treatments, to a final pCO_2 range from ~160–855 µatm at the end of the experiment. ^{13}C-bicarbonate (10 g per mesocosm), corresponding to ~0.1 % of DIC, was added to the mesocosms together with the first CO_2 addition (t_{-1}), increasing the $\delta^{13}C$ signature of DIC by ~100 ‰. At t_{13}, inorganic nutrients were added to stimulate phytoplankton production. The total added concentrations were 5 µM nitrate, 0.32 µM phosphate, and 2.5 µM silicate. The experiment was terminated at t_{30}. The experimental period was divided into three phases based on the applied perturbations and chl *a* dynamics. Phase 1 was before nutrient addition ($t_{4–13}$). Phase 2 was after nutrient addition until the 2nd chl *a* minimum ($t_{14–21}$) and phase 3 was from the 2nd chl *a* minimum until the end of the experiment ($t_{22–29}$) (Schulz et al., 2012). In this manuscript we only consider two phases, phase 1 before nutrient addition ($t_{0–12}$) and phase 2 after nutrient addition ($t_{14–29}$).

BGD
9, 8571–8610, 2012

Depth-integrated samples (0–12 m) were taken with an integrating watersampler (IWS; Hydrobios, Kiel, Germany) on each morning (9–11 h) for most parameters including nutrients, chlorophyll, particulate organic carbon, phosphate, and nitrogen (POC, POP, PON), dissolved organic carbon, phosphate, and nitrogen (DOC, DOP, DON), dissolved inorganic carbon (DIC), ^{13}C content of carbon pools (DIC, DOC, POC, biomarkers). Daily samples for ^{13}C-DIC and ^{13}C-DOC were taken directly from the IWS and stored in dark, gas-tight glass bottles. The sediment traps were emptied every other day before daily routine sampling and processed as described in (Czerny et al., 2012). Zooplankton samples were taken weekly in the afternoon by vertical 55 µm mesh size Apstein net hauls over the upper 12 m.

Daily ^{13}C-polar lipid fatty acid (PLFA) samples were collected on pre-combusted 47 mm GF/F filters by filtering ~3–4 l and filters were stored at −80 °C. Daily ^{13}C-POC samples were collected on pre-weighted and pre-combusted 25 mm GF/F filters by filtering ~0.5 l and filters were subsequently stored at −20 °C and freeze-dried afterwards. From the gas-tight water samples, headspace vials (20 ml) were filled using an overflow method and sealed with gas-tight caps for DIC isotope analyses. Mercury chloride was added for preservation and the samples were stored upside down at room temperature. Samples for dissolved organic carbon (DOC) were GF/F filtered and stored frozen (−20° C) in clean (HCl and mQ rinsed) vials until further analyses. Zooplankton were transferred to filtered seawater and kept there for a minimum of 3 h, to empty their guts. On average, 7 (range 1–30) individuals of *Calanus* sp. and 30 (range 16–35) individuals of *Cirripedia* were handpicked and transferred to pre-combusted tin cups (200 °C, min. 12 h), which were subsequently freeze-dried. Zooplankton samples were analyzed for organic ^{13}C content. Subsamples of freeze-dried and homogenized sediment trap material were analyzed for total organic ^{13}C. Sediment trap material of the last 8 days ($t_{22–30}$) was additionally analyzed for ^{13}C-PLFA to characterize the nature of settling material.

BGD
9, 8571–8610, 2012

2.2 Laboratory analyses

POC, sediment trap material and zooplankton samples were analyzed for organic carbon content and isotope ratios on a Thermo Electron Flash EA 1112 analyzer (EA) coupled to a Delta V isotope ratio mass spectrometer (IRMS). For DIC isotope analyses, a helium headspace was added to the headspace vials and samples were acidified with H_3PO_4 solution. After equilibration, the CO_2 concentration and isotope ratio in the headspace was measured on EA-IRMS. PLFA were extracted using a modified Bligh and Dyer method (Bligh and Dyer, 1959; Middelburg et al., 2000). The lipids were fractionated in different polarity classes by column separation on a heat activated silicic acid column and subsequent elution with chloroform, acetone and methanol. The methanol fractions, containing most of the polar lipid fatty acids were collected and derivatized to fatty acid methyl esters (FAME). The standards 12:0 and 19:0 were used as internal standards. Concentrations and $\delta^{13}C$ of individual PLFA were measured using gas chromatography-combustion isotope ratio mass spectrometry (GC-C-IRMS) (Middelburg et al., 2000; de Kluijver et al., 2010). ^{13}C-DOC samples were analysed in Hatch isotope laboratory (Ottawa, Canada), using wet chemical oxidation with high amplification isotope ratio mass spectrometry (WCO-IRMS) (Osburn and St Jean, 2007). Unfortunately, the amount of ^{13}C was too low to quantitatively determine ^{13}C incorporation in DOC, but could be used to provide an upper limit to DOC production.

2.3 Data analyses

Carbon stable isotope ratios are expressed in the delta notation relative to Vienna Pee Dee Belemnite (VPDB) standard ($\delta^{13}C$). Relative (^{13}C) incorporation in carbon samples is presented as $\Delta\delta^{13}C$ (‰), calculated as $\delta^{13}C_{sample} - \delta^{13}C_{background}$. Absolute label incorporation was calculated as ^{13}C concentration = $\Delta^{13}F \cdot \text{concentration}(\mu\text{mol C l}^{-1})$, with $\Delta^{13}F$ being $^{13}F_{sample} - {}^{13}F_{background}$, and ^{13}F being the ^{13}C fraction ($^{13}C/(^{12}C + {}^{13}C)$) derived from the delta notation. $\delta^{13}C_{background}$

BGD
9, 8571–8610, 2012

and $^{13}F_{background}$ are the natural abundance isotope ratios, which were sampled before label addition. To compare ^{13}C concentrations of organic carbon pools between mesocosms, the data were corrected for small differences in initial ^{13}C DIC concentrations using a correction factor. The correction factor was calculated from deviations of ^{13}C-DIC from the average ^{13}C-DIC on day 3 (after main CO_2 additions) and ranged from 0.89 to 1.08. This correction is used for clarity of presentation and was not used for model calculations. ^{13}C-DIC results were corrected for gas exchange according to (Czerny et al., 2012). The $\delta^{13}C$ of CO_2 (aq) was calculated according to (Zhang et al., 1995) and the $\delta^{13}C$ of atmospheric CO_2 was assumed −8‰ (Fry, 2006).

$\Delta\delta^{13}C$ PLFA of phytoplankton showed 2 responses of ^{13}C incorporation: rapid label incorporation and more graduate label incorporation. Phytoplankton were therefore separated into 2 groups (phyto I and phyto II) (Fig. 1a). The rapidly incorporating PLFA were 18:3ω3, 18:4ω3, 18:5ω3 (12–15), 18:5ω3 (12–16), and 16:4ω3 and their weighted average $(\Delta)\delta^{13}C$ was used to determine $(\Delta)\delta^{13}C$ of phyto I. The PLFA with delayed incorporation were 20:5ω3, 22:6ω3 and 16:4ω1 and their weighted average $(\Delta)\delta^{13}C$ was used to determine $(\Delta)\delta^{13}C$ of phyto II. PLFA presented in phyto I are characteristic for green algae, chrysophytes, prymnesiophytes, and autotrophic dinoflagellates and PLFA of phyto II are characteristic for diatoms and (heterotrophic) dinoflagellates (Cranwell et al., 1988; Dijkman et al., 2009). It was possible to distinguish between autotrophic dinoflagellates and total dinoflagellates, because 18:5ω3 is considered a chloroplast fatty acid, while 22:6ω3 is a cell membrane lipid (Adolf et al., 2007). The branched fatty acids i15:0, ai15:0, and i17:0 were used to characterize heterotrophic bacteria. The last step involved conversion from PLFA biomass to total organic carbon (OC) concentration for each group. The conversion factor for phyto I was 0.06 (sum PLFA/OC), 0.05 (sum PLFA/OC) for phyto II, based on phytoplankton culture and literature values (Dijkman et al., 2006). The conversion factor for bacterial carbon was 0.01 (sum PLFA/OC) (van den Meersche et al., 2004).

BGD
9, 8571–8610, 2012

Group specific daily growth rates (μ, days^{-1}) were calculated according to Dijkman et al. (2009) as

$$\mu(\text{days}^{-1}) = \ln\left(\frac{^{13}C_{\text{concentration}\,t\rightarrow\Delta t}}{^{13}C_{\text{concentration}\,t}}/\text{cf}\right) \quad (1)$$

$$\text{cf} = \text{mean}\left(1 - \frac{\Delta\delta^{13}C_{\text{phyto}\,t}}{\Delta\delta^{13}C_{\text{DIC}\,t}}\right)_{t\rightarrow t+\Delta t} \quad (2)$$

The correction factor (cf) is necessary to correct for label saturation and represents the difference between phyto and DIC labelling ($\Delta\delta^{13}$C) relative to the $\Delta\delta^{13}$C of DIC averaged over the considered growth period for each mesocosm. Primary production rates were calculated as

$$P(\mu\text{mol C l}^{-1}\,\text{days}^{-1}) = \frac{\Delta^{13}F_{\text{phyto}}}{\Delta^{13}F_{\text{DIC}}} \times \frac{C_{\text{phyto}}}{t} \quad (3)$$

2.4 Model

A nutrient-phytoplankton-zooplankton-detritus (NPZD) model amended with isotope values was constructed to quantify carbon fluxes within the plankton food web. The model is based on those of (de Kluijver et al., 2010) and (van den Meersche et al., 2011) and a detailed description of the model and the equations can be found in (van Engeland et al., 2012). The model equations are also found in the supplementary material. The model code is incorporated in an R-package, which is available upon request. Briefly, the concentrations of both ^{12}C and ^{13}C were modelled separately for the following carbon pools: phyto I, phyto II, labile DOC (LDOC), bacteria, zooplankton, detritus, and sedimented OM. The nitrogen pools explicitly described in the model were DIN and DON. Nitrogen fluxes relating to the other pools were calculated from carbon fluxes with a fixed Redfield stoichiometry. POC and PON were calculated in the model as the sum

BGD
9, 8571–8610, 2012

of phyto I and II, bacteria, zooplankton and detritus. Light was used as forcing function for phytoplankton growth. The fractions of ^{13}C and ^{12}C in DIC were used as forcing functions for ^{13}C and ^{12}C incorporation by phytoplankton, but no growth dependency on DIC (or CO_2) was built in the model. Bacterial biomass (based on PLFA; Fig. 1b) and zooplankton biomass (Niehoff et al., 2012) did not show large biomass changes during the experiment and were assumed to stay constant for model simplicity. Half-saturation constants for DOC uptake by bacteria (ε_{DOC}) and zooplankton grazing on phytoplankton (ε_g) were to set low values, with the assumption that substrate limitation was of minor importance.

The model was implemented in the open source software R (R core team, 2012), using the packages FME and deSolve (Soetaert and Petzoldt, 2009; Soetaert et al., 2009). The output of the model was first manually fitted to the data to obtain good parameter fits. The data that were used to fit the model (observed variables) were phyto I, phyto II, bacteria, zooplankton, DIN, DON, POC, PON, and sediment POC and PON. The model was run separately before (phase 1) and after nutrient addition (phase 2). For both phases initial conditions were based on the data. The fitted parameters were calibrated using the Markov Chain Monte Carlo (MCMC) technique (Gelman et al., 1996), as implemented in the FME package. A subset of parameters, potentially CO_2 sensitive, was calibrated with MCMC for each mesocosm. MCMC runs were accepted when they fell into the probability distribution centred around the current value (for details see Gelman et al., 1996). The model was run 5000 times for each mesocosm, resulting in ~2000 accepted runs. The mean and standard deviation of the MCMCs were calculated for each parameter. The calibrated parameters were used to calculate fluxes ($\mu mol\,C\,l^{-1}\,days^{-1}$) between the carbon pools.

2.5 Statistics

Simple Pearson correlation tests were used to test the effect of CO_2 on growth rates (Eq. 1), production rates (Eq. 3), linear increase in ^{13}C concentrations, and parameters and fluxes derived from the model. The results were tested and plotted against the

BGD
9, 8571–8610, 2012

average pCO_2 level in the corresponding phase. All statistical analyses were done in the software R.

3 Results

3.1 ^{13}C-DIC dynamics

Addition of ^{13}C bicarbonate together with the first CO_2 addition on t_{-1} caused an increase in δ^{13}C of DIC of 117 ± 6 ‰ in all mesocosms (Fig. 1a). The decrease in $\Delta\delta^{13}$C-DIC in perturbed mesocosms during the first 4 days (t_{0-4}) can be largely explained by exchange with the dead volume, which was the space between the sediment traps and the bottom of the mesocosms and comprised ~10 % of total mesocosm volume (Schulz et al., 2012). Other processes that contributed to the initial label decrease were the subsequent (unlabelled) CO_2 additions which diluted the ^{13}C-DIC pool and respiration of unlabeled organic material. The loss of ^{13}C-DIC due to air-sea exchange was low (<0.15 %). From day 7 onwards, the $\Delta\delta^{13}$C of DIC remained quite stable (Fig. 1a). The labelled DIC concentrations were 2.6 ± 0.1 µmol ^{13}C l^{-1} at t_0 and decreased during the first 9 days to 2.2 ± 0.2 µmol ^{13}C l^{-1} at t_{10} and did not show large changes afterwards (Fig. 2a).

3.2 Phytoplankton dynamics

After enclosure of post-bloom water, a phytoplankton bloom developed, even though nutrient concentrations were low (0.64 and 0.05 µmol l^{-1} DIN and phosphate, respectively). Phyto I rapidly incorporated ^{13}C; on t_7 the whole phytoplankton community had been turned-over, as indicated by the plateau (Fig. 1a), although phyto I never reached the $\Delta\delta^{13}$C of DIC. Phyto II showed clearly slower enrichment and never became saturated with ^{13}C (Fig. 1a). Phyto I initially had low biomass (1.2 ± 0.05 µmol C l^{-1}, ~6 % of POC) compared to phyto II (8.3 ± 1.2 µmol C l^{-1}, ~40 % of POC) (Fig. 1b). Both groups

BGD
9, 8571–8610, 2012

contributed to the bloom during phase 1 in biomass and reached a bloom peak at t_6 and declined afterwards (Fig. 1b). The development of ^{13}C labelled biomass showed that the bloom build-up and decline were more pronounced for phyto I compared to phyto II (Fig. 2b, c). This was also reflected in higher growth rates ($0.85 \pm 0.06\,days^{-1}$) of phyto I (μ_I) compared to phyto II (μ_{II}, $0.48 \pm 0.04\,days^{-1}$) during bloom build-up (t_{0-6}). (Table 1). The height of the bloom peak, as well as growth rates of phyto I and phyto II were independent of CO_2.

The production rates (P) of phyto I during the build-up (t_{0-6}) were 0.56–$0.78\,\mu mol\,C\,l^{-1}\,days^{-1}$ and independent of CO_2 (Fig. 3a). Average net production rates in total phase 1 (t_{0-12}) were much lower, $0.09–0.30\,\mu mol\,C\,l^{-1}\,days^{-1}$ and showed a positive relation with CO_2 (Fig. 3a, $r = 0.81$, $p < 0.01$). The production rates of phyto II during the build-up (t_{0-6}) were $0.45–0.62\,\mu mol\,C\,l^{-1}\,days^{-1}$and showed a negative correlation with CO_2 (Fig. 3b, $r = -0.79$, $p < 0.05$). Net production rates of phyto II were $0.21–0.37\,\mu mol\,C\,l^{-1}\,days^{-1}$and were independent of CO_2 (Fig. 3b). So both phytoplankton groups had a significant loss in (particulate) production (ΔP) during the bloom collapse, which was CO_2 dependent. The loss in (particulate) organic carbon production (ΔP) during the collapse, was $\sim 0.39\,\mu mol\,C\,l^{-1}\,days^{-1}$in high and $\sim 0.97\,\mu mol\,C\,l^{-1}\,days^{-1}$in low CO_2 treatments ($r = -0.70$, $p < 0.05$, Fig. 3c).

After nutrient addition phyto I and II increased again in biomass, but there was more variation between mesocosms. Bloom peaks of phyto I were reached on t_{18-29}, depending on the mesocosm, but not on CO_2 (Fig. 2b). Bloom peaks of phyto II were reached on t_{22-29} and were also independent of CO_2 (Fig. 2c). Although ^{13}C biomass of phyto II kept increasing, the total biomass of phyto II after nutrient addition remained similar to phase 1 (Fig. 1b). Average growth and production rates of phyto II after nutrient addition were also similar to phase 1 (Table 1). Production rates of phyto II were initially higher in the high CO_2 treatments (t_{14-22}, $r = 0.72$, $p < 0.05$, Fig. 3d). However, overall production rates in phase 2(t_{14-29}) showed an optimum around current CO_2 levels (Fig. 3d). Because of label saturation (Fig. 1a), growth and production rates could not be determined for phyto I after nutrient addition.

BGD
9, 8571–8610, 2012

3.3 POC and DOC production

The dynamics of phyto I and phyto II were reflected in the build-up of ^{13}C enriched POC with a peak on $t_{8–11}$ and a subsequent decline (Fig. 2d). POC dynamics were independent of CO_2 in phase 1. Addition of nutrients again stimulated organic matter production and ^{13}C-POC kept on increasing until the end of the experiment (Fig. 2d). POC production rates before and after nutrient addition were quite similar: 0.65–1.06 µmol C l^{-1} $days^{-1}$ before and 0.57–1.06 µmol C l^{-1} $days^{-1}$ after nutrient addition (Table 1, Fig. 4a). The average production rate of POC after nutrient addition ($t_{14–29}$) decreased with increasing CO_2 ($r = -0.87$, $p < 0.01$, Fig. 4a). DO^{13}C showed a maximum increase ($\Delta\delta^{13}C$) of 3‰ . Based on the small isotopic enrichment, the average DOC production during the whole experiment ($t_{0–28}$) was <0.06 µmol C l^{-1} $days^{-1}$ and the total DOC build-up was <6.2 µmol C l^{-1} in phase 1 ($t_{0–11}$) and <11 µmol C l^{-1} in phase 2 ($t_{14–28}$).

3.4 ^{13}C labelling of bacteria and zooplankton consumers

Heterotrophic (gram-positive) bacterial followed the labelling pattern of POC (Fig. 1a). Initial bacteria biomass was 4.6 ± 0.6 µmol C l^{-1} (~19 % of POC) and stayed constant during phase 1 (Fig. 1b). Due to label incorporation, the ^{13}C-enriched bacteria biomass increased in the first phase and peaked on $t_{6–8}$ (Fig. 2e). Bacteria ^{13}C biomass increased again after nutrient addition until the end of the experiment. The average growth rate of bacteria (μ_{Bac}) was 0.33 ± 0.02 $days^{-1}$ before nutrient addition and 0.13 ± 0.04 $days^{-1}$ after nutrient addition (Table 1). Bacteria production rates were also higher before nutrient addition (phase 1, 0.47 ± 0.03 µmol C l^{-1} $days^{-1}$) than after nutrient addition (phase 2, 0.20 ± 0.15 µmol C l^{-1} $days^{-1}$) (Table 1). Bacteria growth and production were independent of CO_2 levels.

Zooplankton (*Calanus* sp. and *Cirripedia*) incorporated ^{13}C in a similar way and the incorporation of tracer into copepods was used as representative for

BGD
9, 8571–8610, 2012

the mesozooplankton community. The ^{13}C incorporation into zooplankton was low (Fig. 1a). With a constant biomass of ~5 µmol C l^{-1} (Niehoff et al., 2012), the ^{13}C incorporation until day 18 showed a negative correlation with CO_2 ($r = -0.92$, $p < 0.001$, Figs. 2f, 4b). From day 24 onwards, the variance in ^{13}C biomass increased and the CO_2 effect disappeared (Fig. 2f).

3.5 ^{13}C labelling of sedimented organic material

The label enrichment in sediment trap organic matter in the first 7 days was low, indicating that little freshly produced material was sinking into the traps (Fig. 1a). After day 7 the material became more enriched, probably because of the bloom collapse and after day 20, the $\Delta\delta^{13}C$ of sediment trap POC increased rapidly (Fig. 1a). After day 25, the $\Delta\delta^{13}C$ of sediment POC was higher than of water column POC, showing that there was preferential sinking of freshly produced material. The cumulative ^{13}C of sediment trap POC is shown in Fig. 2g. The settling of ^{13}C enriched POC in the traps was very low in the first phase (7.13×10^{-6} µmol ^{13}C l^{-1} $days^{-1}$, ~7.13×10^{-3} µmol C l^{-1} $days^{-1}$) and increased with increasing CO_2 ($r = 0.75$, $p < 0.05$, Fig. 4c). After nutrient addition, the sinking of ^{13}C-POC was much higher (1.14×10^{-4} µmol ^{13}C l^{-1} $days^{-1}$, ~0.11 µmol C l^{-1} $days^{-1}$) and the effect of CO_2 on sedimentation was reversed compared to phase 1 (Figs. 2g, 4c); sedimentation of freshly labeled (^{13}C enriched) POC decreased with increasing CO_2 ($r = -0.78$, $p < 0.05$, Fig. 4c). The ^{13}C increase in POC in the water column and sediment traps showed a non-linear response to CO_2 in phase 2, which indicates a step-wise rather than a gradual CO_2 effect (Fig. 4a, c). Mesocosms with CO_2 levels below 340 µatm had high POC production and sedimentation rates, while mesocosms with CO_2 above 400 µatm had low POC production and sedimentation rates after nutrient addition (Fig. 4a, c). The exception was at 395 µatm (average pCO_2 in phase 2 in mesocosm 8) where there was high production and low sedimentation (Fig. 3d, f). The fatty acid composition of settling material in phase 3

BGD
9, 8571–8610, 2012

revealed that all groups were present, but there were more phyto II markers than phyto I markers in the sediment traps.

3.6 Model results: parameters

The construction of a model and subsequent fitting to the data provides the possibility to study the community as a whole, instead of studying carbon production in each carbon pool separately as done above. Good model fits were obtained for the first phase of the model (t_{0-12}). Unfortunately, no good fits could be obtained for phase 2 (t_{14-29}), primarily because of label saturation in phyto I (Van Engeland et al., 2012) which precluded fitting the growth rate and subsequent exudation and mortality of phyto I during this phase. Fits for phase 1 of one mesocosm (M4, 375 µatm) are shown in Fig. 5 and the fits for the other mesocosms can be found in the supplementary material A. The average parameter values of all mesocosms are given in Table 2. The growth and build-up of plankton biomass caused a decrease in DIN and DON. To reach the high biomass of phyto I, phytoplankton mortality was set to 0 in the first six days. The growth rate of phyto I (μ_{I}) was $0.87 \pm 0.013\,\mathrm{days}^{-1}$. After t_6 phytoplankton mortality was included to produce the decline in biomass. The mortality rate of phyto I (ξ_{I}) was $0.29 \pm 0.081\,\mathrm{days}^{-1}$. The growth rate of phyto II (μ_{II}) was $0.18 \pm 0.010\,\mathrm{days}^{-1}$. The estimated loss rate of phyto II (ξ_{II}) was low, only $0.045 \pm 0.025\,\mathrm{days}^{-1}$. Hence mortality mainly affected phyto I. Part of the phytoplankton loss was assumed to be respired, part to end up in DOM, and part to end as detritus. The loss part that went into detritus (f_{Det}) was 0.37 ± 0.050 and the part that ended in DOM (f_{DOM}) was 0.056 ± 0.037, meaning that the rest (0.57) of the dead material was respired into the DIC pool (Table 2). Both phytoplankton groups exudated DOM that was assumed to have the isotope signature of phytoplankton. The exudation rate of phytoplankton I (γ_{I}) was $0.31 \pm 0.023\,\mathrm{days}^{-1}$ and the exudation rate of phyto II (γ_{II}) was $0.24 \pm 0.017\,\mathrm{days}^{-1}$. No build-up of labile DOC (LDOC) was observed, because the freshly produced DOM was rapidly consumed by bacteria. Bacteria biomass was assumed constant (Fig. 1b),

BGD
9, 8571–8610, 2012

meaning that growth and loss (respiration/mortality/grazing) were balanced. Bacteria maximum growth (μ_{Bac}) was $0.36 \pm 0.029\,days^{-1}$. Mesozooplankton was assumed to graze on phytoplankton and low grazing rates for zooplankton (μ_g) were observed, only $0.022 \pm 0.005\,days^{-1}$ and the fraction of grazing that went into faeces (f_{faeces}) was 0.15. Zooplankton biomass in the mesocosms stayed constant, but a large number of zooplankton (*Cirripedia*) was found in the sediment traps (Niehoff et al., 2012; Czerny et al., 2012). The part of zooplankton losses (which balanced zooplankton gains) that ended in the traps (ξ_{Zoo}) was 65 % and the other 35 % was respired. Detritus was mainly formed of dead phytoplankton, so started to increase after day 6, when mortality of phytoplankton occurred. The mineralisation rate (ρ) of detritus into DIN and DIC was $0.020 \pm 0.004\,days^{-1}$ and sinking rate of detritus (r_{sink}) was $0.008 \pm 0.005\,days^{-1}$ (Table 2). Two of the twelve model parameters potentially sensitive to CO_2 showed to be indeed affected by CO_2 treatments. Grazing rates (μ_g) decreased with increasing CO_2 (Fig. 6a, $r = -0.79$, $p < 0.05$). Sinking rates (r_{sink}) showed a positive correlation with pCO_2 ($r = 0.81$, $p < 0.01$, Fig. 6b). The sinking was 5 times higher at high CO_2 ($0.016 \pm 0.0034\,days^{-1}$) compared to lower CO_2 ($0.0020 \pm 0.0014\,days^{-1}$). For validation of the parameters, the model was also tested with ξ_{Zoo} included as CO_2 sensitive parameter. ξ_{Zoo} is the part of zooplankton carbon gain that ended in the sediment traps. ξ_{Zoo} was found to be CO_2 independent. The amount of zooplankters that ended in the traps were also independent of CO_2 levels (Niehoff et al., 2012). As including the parameter increased the model uncertainty it was therefore excluded from MCMC analysis.

3.7 Model results: carbon fluxes

The set of parameters that was selected during the MCMC analysis was used to calculate average carbon fluxes over phase 1 (t_{0-12}). The flux from DIC to phytoplankton was $1.78 \pm 0.17\,\mu mol\,C\,l^{-1}\,days^{-1}$, with a flux of $1.17 \pm 0.10\,\mu mol\,C\,l^{-1}\,days^{-1}$ to phyto I and a flux of $0.61 \pm 0.089\,\mu mol\,C\,l^{-1}\,days^{-1}$ to phyto II (Fig. 7). Large parts from

BGD
9, 8571–8610, 2012

gross phytoplankton production were exudated as DOC, $0.36 \pm 0.05\,\mu mol\,C\,l^{-1}\,days^{-1}$ and $0.19 \pm 0.03\,\mu mol\,C\,l^{-1}\,days^{-1}$ from phyto I and II, respectively, so $0.59 \pm 0.06\,\mu mol\,C\,l^{-1}\,days^{-1}$ in total, and $30.7 \pm 1.2\%$ of total primary production. DOC was assumed to be the only carbon source for bacteria and the consumption rate of bacteria was $0.60 \pm 0.062\,\mu mol\,C\,l^{-1}\,days^{-1}$. The small discrepancy between DOC production and bacteria production was covered by an initial decrease in LDOC. Over phase 1, the ratio of bacterial production to primary production (BP:PP) was 0.34 ± 0.032. The carbon consumption of zooplankton was much lower, only $0.19 \pm 0.04\,\mu mol\,C\,l^{-1}\,days^{-1}$ from which $0.028 \pm 0.007\,\mu mol\,C\,l^{-1}\,days^{-1}$ went into faeces. Zooplankton consumed equal parts from phyto I and phyto II, because similar grazing efficiency on phytoplankton was assumed (Fig. 7). The fractions of primary production channelled into zooplankton production were $7.4 \pm 1.8\%$ and $16.7 \pm 4.1\%$ for phyto I and II, respectively. Because grazing rates were CO_2 sensitive (Fig. 5a), the carbon flows from phytoplankton to zooplankton were also CO_2 sensitive as indicated by the dashed lines (Fig. 7). The mortality carbon flow was $0.60 \pm 0.062\,\mu mol\,C\,l^{-1}\,days^{-1}$ for phyto I, i.e. $51.3 \pm 7.0\%$ of primary production. Mortality carbon flow of phyto II was only $0.21 \pm 0.11\,\mu mol\,C\,l^{-1}\,days^{-1}$ or $36.2 \pm 19.8\%$ of primary production. From the total carbon flow of dead phytoplankton ($0.81 \pm 0.16\,\mu mol\,C\,l^{-1}\,days^{-1}$), $0.044 \pm 0.029\,\mu mol\,C\,l^{-1}\,days^{-1}$ went into DOM, $0.47 \pm 0.093\,\mu mol\,C\,l^{-1}\,days^{-1}$ into respiration and $0.30 \pm 0.074\,\mu mol\,C\,l^{-1}\,days^{-1}$ into detritus (Fig. 7). The carbon flow of detritus export was low, only $0.021 \pm 0.093\,\mu mol\,C\,l^{-1}\,days^{-1}$. Because sinking rates were CO_2 sensitive, the flow from detritus to sediment traps was also CO_2 sensitive, as indicated by the dashed line in Fig. 7. The total carbon flow into the sediment traps was $0.13 \pm 0.018\,\mu mol\,C\,l^{-1}\,days^{-1}$, so the majority came from zooplankton (Fig. 7). The export of primary production was only $7.1 \pm 1.4\%$, indicating a retention food chain rather than an export food chain.

BGD
9, 8571–8610, 2012

4 Discussion

4.1 Plankton carbon flows under low nutrients

While most of the CO_2 enrichment mesocosm experiments involved inorganic nutrient addition and focussed on production and export food chains, this study investigated ocean acidification in a nutrient regenerating food chain, at least during phase 1 of the experiment. The low nutrient concentrations, low chl *a*, and high heterotrophic biomass in Kongsfjorden waters were characteristic for a post-bloom situation (Rokkan-Iversen and Seuthe, 2011). Although nutrient concentrations were low, a small phytoplankton started right after enclosure, probably fuelled by efficient recycling of nutrients accompanied with remineralisation of DON. Total primary production rates in our experiment (21 mmol C m^{-2} $days^{-1}$, integrated over the 12 m sampling depth) were similar to the median particulate primary production of 20 mmol C m^{-2} $days^{-1}$ in Arctic regions (synthesis by Kirchman et al., 2009a). However, particulate primary production in this study was lower, ~14 mmol C m^{-2} $days^{-1}$ (integrated over the 12 m sampling depth), suggesting nutrient limitation in our study. The primary production during the bloom was dominated by autotrophs or nanoplankton (comprised in phyto I) as indicated by their high growth and production rates (Tables 1, 2). Despite their low biomass, they were responsible for two thirds of the primary production in phase I. The other third of primary production was contributed by phyto II. Although phyto II dominated in terms of biomass, they had lower growth and production rates, likely attributable to the mixotrophic character of the group. The difference in model based primary production and data based particulate primary production is the dissolved primary production: exudation of recent fixed organic matter. Two thirds of GPP was used for net particulate primary production (1.2 µmol C l^{-1} $days^{-1}$, Table 1) and the other one third was exuded as dissolved primary production to fuel bacterial production. Bacteria were an important component of the pelagic food web and a rapid consumer of primary production, as indicated by rapid transfer of label from phytoplankton to bacteria (Fig. 1a). Bacteria production amounted to a third of total phytoplankton production (34 %). A remarkably similar average BP:PP

BGD
9, 8571–8610, 2012

ratio (34 %) was observed in Arctic transect studies by Kirchman et al. (2009b), although their absolute production rates were much lower. In a data synthesis by (Cole et al., 1988), the BP:PP in the euphotic zone was typically 20–30 %. Bacterial growth rates in phase 1 (0.33–0.36 $days^{-1}$) were relatively high compared to average Arctic bacterial growth rates (Kirchman et al., 2009a). Despite the high growth rates, the biomass of bacteria did not increase (Fig. 1b), indicating a strong removal pressure (top-down control) on bacteria e.g. by viruses or microzooplankton (heterotrophic dinoflagellates) grazing. The high abundance of heterotrophic dinoflagellates indicates that microzooplankton grazing likely controlled bacterial biomass (Schulz et al., 2012). Also mesozooplankton had high biomass, but grazing rates of mesozooplankton on primary production were very low, as indicated by maximum daily grazing rates of 0.022 $days^{-1}$ on phytoplankton biomass. In phase 1, only 11 % of primary production was consumed by mesozooplankton. Summarized, the high BP:PP, high microzooplankton abundance, and low mesozooplankton grazing indicate that the microbial food web was more important in this study than a herbivorous food web (Legendre and Razouldagan, 1995). Our results on plankton food web structure fit very well with the previously described post-bloom (May–July) situation in Kongsfjorden (Rokkan Iversen and Seuthe, 2011) with high BP:PP production and a prominent role for the microbial food web. However, they suggested a control of phytoplankton biomass by mesozooplankton grazing, because of low phytoplankton biomass, high primary production, and high zooplankton biomass, which is not supported by our findings. Viral infections likely caused the bloom to collapse after t_6, since phytoplankton decline coincided with a peak in virus abundance (Brussaard et al. 2012). Mortality affected phyto I much more than phyto II, consistent with virus-host specificity. Phytoplankton mortality rates of up to 0.3 $days^{-1}$, as observed for phyto I, have been recorded during bloom declines as well as in oligotrophic systems (reviewed in Brussaard, 2004). When phytoplankton cells die, the cells lyse and a large portion is released into DOM, which can be subsequently used by bacteria (reviewed in Brussaard, 2004). In our study, phytoplankton mortality did not stimulating bacterial production per se, since bacterial production declined after

BGD
9, 8571–8610, 2012

6 as well. Possible explanations for the decline in bacterial production are concurrent viral infections or a shift from microzooplankton grazers from phyto I to bacteria. DOC accumulation after mortality was observed in the mesocosms (Czerny et al., 2012; Engel et al., 2012). The material released by viral lysis is sticky and viral induced mortality can enhance formation and persistence of large aggregates (Peduzzi and Weinbauer, 1993). Although it was difficult to constrain, we estimated that approximately one third of dying phytoplankton ended up as detritus. Detritus formed only a small part of total POC (10 %) and was thus mainly formed of dead algae. The sedimentation losses of detritus were low (0.008 $days^{-1}$) and in phase 1, sinking detritus comprised only 1 % of primary production. In phase 1, zooplankton contributed substantially to sedimented organic material (Niehoff et al., 2012). Together with zooplankton settling in the traps, the average export corresponded to ~ about 7 % of primary production. In contrast, the calculated export in a previous mesocosm experiment with nutrient addition was ~24 times higher than the export rates in this experiment (Riebesell et al., 2007).

4.2 Plankton carbon flows after nutrient addition

The addition of nutrients did not increase phytoplankton and bacterial biomass in the mesocosms (Fig. 1b). However, chl *a* increased after nutrient addition (Schulz et al., 2012), indicating that phyto II shifted towards an autrophic community. The production rate of phyto II also slightly increased after nutrient addition (Table 1). Interestingly, bacterial production and growth decreased after nutrient addition (Table 1), contrary to the generally observed positive relation between nutrient concentrations and growth efficiency (del Giorgo and Cole, 1998). Bacteria in phase 2 could have been limited by substrate (DOC) availability, since extra cellular release decreased after nutrient addition (Engel et al., 2012). In agreement with our findings, a similar decrease in bacterial growth after nutrient addition was found with radioactive leucine incorporation during the experiment (Piontek et al., 2012). The largest change in phase 2 compared to phase 1 was an increase in sedimentation. Large sedimentation of (freshly produced) organic matter occurred after day 24, when chain-forming diatoms started to dominate

BGD
9, 8571–8610, 2012

the mesocosms (Czerny et al., 2012). The diatoms probably formed aggregates that facilitated sinking of organic matter. The higher isotopic enrichment of sedimented organic matter compared to the water column (Fig. 1a) showed that the aggregates were formed of freshly produced organic matter and the dominance of diatoms was confirmed by the high presence of phyto II markers in the sediment trap material.

4.3 Methodological considerations and assumptions

^{13}C labelling combined with modelling has been used successfully in previous mesocosm studies to quantify carbon flows and interactions in plankton food webs (van den Meersche et al., 2004, 2011; de Kluijver et al., 2010). However, there are some assumptions and potential errors that need attention. A main advantage of using a ^{13}C tracer is that production can be measured in situ, in contrast to other methods like radioactive tracers that require side incubations with perturbed environmental (e.g. light) conditions. Using PLFA biomarkers, phytoplankton and bacteria group specific primary production can be estimated in addition to total POC production (Dijkman et al., 2009). However, PLFA based production (phyto I, II, bacteria) slightly overestimated the production of total POC (Table 2), what can be explained by potential errors in conversion factors and uncertainties arising from averaging numbers. A comparison of community production measurements performed during the experiment with different methods (DIC, oxygen, ^{14}C, ^{13}C) is presented by (Tanaka et al., 2012). There was a good correlation between ^{13}C-POC and DIC based NCP, as we expected, since they were both measured in situ (Tanaka et al., 2012).

Although PLFA can be used as taxonomic markers (Dijkman and Kromkamp, 2006) the majority of PLFA markers do not allow distinction between heterotrophic and autotrophic phytoplankton, like mixotrophic dinoflagellates, and therefore we had to consider heterotrophic dinoflagellates as part of phyto II. Phyto II had the largest biomass (36 % of POC) and comparison with chl *a* as a proxy for autotrophic biomass, after subtraction of phyto I, indicated that >65 % of phyto II in phase I was heterotrophic (Czerny et al., 2012). The ^{13}C incorporation method is limited when phytoplankton is saturated

BGD
9, 8571–8610, 2012

with tracer, i.e. it has taken the signature of the source, corrected for fractionation, in which case uptake of substrate will not cause further changes in ^{13}C. Saturation was observed in phyto I after the first six days precluding growth estimates after this period and precluding model application for phase II. For future experiments an additional ^{13}C spike with nutrient addition is recommended (van Engeland et al., 2012). The other carbon pools did not get saturated with tracer (Fig. 1a) and bacteria never reached the isotope labelling of phytoplankton (Fig. 1a). Assuming that phytoplankton is the only carbon source for bacteria, this implies a senescent or dorming pool of bacteria that did not grow during the experiment. Another explanation is that bacteria grew on total POC, which is likely, since they closely followed the labelling of POC (Fig. 1a). Zooplankton never reached label enrichment of any carbon pool (Fig. 1a). Mesozooplankton has a slow turnover in response to dietary changes, what contributes to low labelling patterns. A study on carbon turnover in Arctic crustaceans showed low turnover in stable isotopes, with a half life of 14 days (Kaufman et al., 2008). For simplicity, one grazing rate on phytoplankton was assumed in the model, but there was probably selective grazing on different phytoplankton groups. Due to the labelling differences between phyto I and II, grazing rates would decrease if zooplankton primarily grazes on phyto I and increase if zooplankton primarily grazes on phyto II.

Production processes are relatively easy to determine with ^{13}C incorporation, but it is more challenging to quantify and allocate loss processes. The partitioning of carbon from phytoplankton mortality was difficult to constrain (van Engeland et al., 2012). The partitioning in the particulate fraction was relatively easy to determine, because of direct POC measurements, but partitioning into dissolved material was more difficult, because of lack of accurate ^{13}C-DOC measurements. Measuring isotope labelling in DOC is challenging because of methodological constraints (Osburn and St Jean, 2007; van den Meersche et al., 2011) and because of the high background concentrations of total DOC (4 times POC). Moreover, it is expected that freshly produced DOC is rapidly consumed rather than accumulating in the DOC pool. DOC production derived from the model to fuel bacteria production was 10 times higher than DOC production based

BGD
9, 8571–8610, 2012

on ^{13}C incorporation. For sufficient ^{13}C enrichment in DOC, the amount of added tracer should be >10 times higher.

The data from the sediment trap samples have to be considered with care. The sediment traps were positioned only ~15 m deep, so the material in the sediment traps cannot quantitatively considered to be exported compared to studies were traps were placed below the euphotic zone. The sediment traps were also within the daily migration zone of zooplankton and there were a large number of *Cirripedia* settling in the sediment traps. Zooplankton can contribute largely to settling material, especially in shallow traps and contributions of 14–90 % of zooplankton to POC in traps were reported by Buesseler et al. (2007). In the model a 82 % contribution of zooplankton to sediment trap material was necessary to achieve the low labelling of sediment material in phase 1. Preferential settling of old, unlabeled material in the traps could have contributed to the low labelling as well, but this was not considered in the model. Although above processes can cause potential errors in the estimated carbon fluxes, they do not explain the observed CO_2 effects, since they are expected to occur in all mesocosms.

4.4 CO_2 effects

In this study, we aimed to increase our understanding of CO_2 effects on primary production, community respiration, and export in Arctic communities by looking at individual uptake and loss rates and by quantifying the interactions between food web compartments with a food web model. Some of the CO_2 effects in phase 1 that were observed in individual fluxes (grey arrows in Fig. 7) were not shown in the integrated food web, so we consider them with care.

Although it was not captured by the model, the data suggest that loss in phytoplankton production due to mortality can be CO_2 sensitive. When the bloom collapsed (after t_6), the loss in particulate primary production was significantly lower at higher CO_2 levels (Fig. 3c). Furthermore, both simple regression (Fig. 4c) and model inference (Fig. 6b) showed that sedimentation of fresh organic matter increased with increasing

BGD
9, 8571–8610, 2012

CO_2. These observations suggest the presence of CO_2 effects on phytoplankton mortality in phase 1. Since mortality rates were not sensitive to CO_2 and viral numbers were not CO_2 dependent (Brussaard et al., 2012), we speculate that there were CO_2effects on the partitioning of dead phytoplankton in particulate and dissolved organic matter fractions. The organic material released at high CO_2 could be of more sticky nature serving as precursor of transparent exopolymer particles (TEP) or less degradable (Engel et al., 2002; Czerny et al., 2012; Engel et al., 2012). When more phytoplankton mortality ends in aggregates or particles, it could lead to enhanced sinking at high CO_2, as observed in phase 1. Future research on CO_2 effects on partitioning of phytoplankton mortality is needed to support our hypotheses.

Both simple regression (Fig. 4b) and model output (Fig. 6a), showed reduced zooplankton grazing in phase I with increasing CO_2. There was no CO_2 effect found on zooplankton numbers (Niehoff et al., 2012) and we can only speculate about the mechanisms. One potential explanation is that reduced grazing is a direct consequence of higher sedimentation at higher CO_2 during phase 1. Reduced grazing could also result from the reduced initial production of phyto II at higher CO_2 (Fig. 3b). Other possible explanations for reduced grazing could be CO_2 induced changes in food quality, i.e. the production of less essential fatty acids. However, there were no CO_2 dependent shifts in fatty acid compositions observed in phase 1 (this study, Leu et al., 2012). A hampering CO_2 effect on *Cirripedia* development to the next stage was observed (Niehoff et al., 2012), but whether this was related to lower grazing, needs to be further addressed.

In this study, no CO_2 effect on bacteria growth and production were observed. There was also no CO_2 effect on carbon exudation by phytoplankton as source for bacteria, although this process is considered potentially CO_2 sensitive. It has been hypothesized that increasing CO_2 could stimulate carbon overconsumption and subsequent extracellular release, but most studies done so far showed no effects on DOC production in community-level CO_2enrichment studies (e.g., Engel et al., 2004b). Previous mesocosm studies focussed on nutrient replete situations and it was suggested that CO_2 effects on extracellular release would be more pronounced under nutrient limitation

BGD
9, 8571–8610, 2012

(Thingstad et al., 2008; de Kluijver et al., 2010). The results here show that bacterial production on phytoplankton exudation is also not enhanced with CO_2 in a post bloom situation. However, when bacterial growth is limited by nutrient availability, a lack of bacterial response does not necessary mean that there was no stimulation of extracellular release. Exudates are also important players in formation of TEP and marine snow and subsequent export (Engel et al., 2004a).

After nutrient addition phytoplankton production (phyto II) was initially stimulated by higher CO_2($t_{14–22}$), but showed an optimum around current CO_2 levels of 340 µatm over the whole phase after nutrient addition ($t_{14–28}$; Fig. 3c). The response of phyto II was likely an indirect effect of CO_2 due to competition with other phytoplankton groups. The proposed mechanism (based on pigments and flow cytometry) is that increasing CO_2 stimulated production of picoplankton directly after nutrient addition and outcompeted larger phytoplankton like diatoms in the final stage of the experiment (Schulz et al., 2012). The response to CO_2 after nutrient addition was also not gradual for POC production and sedimentation. POC production after nutrient addition showed a non-linear response to CO_2 with a transition point around current CO_2 levels (Fig. 4a). Production was lower at CO_2levels above 400 µatm and because of the large export in phase 3, the CO_2 effect on POC production was directly reflected in settling material (Fig. 4c). Our findings suggest that CO_2 effects on some processes are stepwise rather than gradual, which can be of interest for future research.

5 Conclusions

This mesocosm study is the first to study ocean acidification effects on Arctic plankton communities, in a system dominated by regenerated production. Before nutrient addition (phase 1) the pelagic food web was characterized by high BP:PP, high microzooplankton abundance, low mesozooplankton grazing and low export. Comparable production rates, but increased export were observed after nutrient addition (phase 2). CO_2 effects were subtle and different for each phase. We observed a stimulating effect

BGD
9, 8571–8610, 2012

of CO_2 on export and a hampering effect on community (mesozooplankton) respiration in phase 1 and a hampering effect of CO_2 on production and export in phase 2. Generally, more research on plankton communities with different composition and nutrient states are necessary to improve our understanding of pelagic food web processes under future CO_2 conditions.

Acknowledgements. This work is a contribution to the "European Project on Ocean Acidification" (EPOCA) which received funding from the European Community's Seventh Framework Programme (FP7/2007–2013) under grant agreement no. 211384. We gratefully acknowledge the logistical support of Greenpeace International for its assistance with the transport of the mesocosm facility from Kiel to Ny-Ålesund and back to Kiel. We also thank the captains and crews of M/V *ESPERANZA* of Greenpeace and R/V *Viking Explorer* of the University Centre in Svalbard (UNIS) for assistance during mesocosm transport and during deployment and recovery in Kongsfjorden. We thank the staff of the French-German Arctic Research Base at Ny-Ålesund, in particular Marcus Schumacher, for on-site logistical support. We thank the Dutch Station and especially Maarten van Loon for accommodation in Ny-Ålesund. We thank the mesocosm team and especially the people of GEOMAR for their support during the experiment. The excellent team spirit made the experiment enjoyable and successful. We thank Pieter van Rijswijk of NIOZ for preparation and lab support. The analytical lab at NIOZ is acknowledged for stable isotope analyses. We thank Richard Bellerby of Bjerknes Centre for Climate Research for the provision of DIC numbers. Mehdi Ghourabi is acknowledged for his help with model construction. Financial support was provided through Transnational Access funds by the EU project MESOAQUA under grant agreement no. 22822, the European Project on Ocean Acidification (EPOCA, FP7, 2211384), and the Darwin Center for Biogeosciences supported by the Netherlands Organization for Scientific Research.

Supplementary material related to this article is available online at: http://www.biogeosciences-discuss.net/9/8571/2012/bgd-9-8571-2012-supplement.pdf.

BGD
9, 8571–8610, 2012

References

Adolf, J. E., Place, A. R., Stoecker, D. K., and Harding, L. W.: Modulation of polyunsaturated fatty acids in mixotrophic Karlodinium veneficum (*Dinophyceae*) and its prey, *Storeatula* major (*Cryptophyceae*)1, J. Phycol., 43, 1259–1270, doi:10.1111/j.1529-8817.2007.00419.x, 2007.

Allgaier, M., Riebesell, U., Vogt, M., Thyrhaug, R., and Grossart, H.-P.: Coupling of heterotrophic bacteria to phytoplankton bloom development at different pCO_2 levels: a mesocosm study, Biogeosciences, 5, 1007–1022, doi:10.5194/bg-5-1007-2008, 2008.

Bellerby, R. G. J., Schulz, K. G., Riebesell, U., Neill, C., Nondal, G., Heegaard, E., Johannessen, T., and Brown, K. R.: Marine ecosystem community carbon and nutrient uptake stoichiometry under varying ocean acidification during the PeECE III experiment, Biogeosciences, 5, 1517–1527, doi:10.5194/bg-5-1517-2008, 2008.

Bellerby, R. G. J., Silyakova, A., Nondal, G., Slagstad, D., Czerny, J., De Lange, T., and Ludwig, A.: Marine carbonate system evolution during the EPOCA Arctic pelagic ecosystem experiment in the context of simulated future Arctic ocean acidification, in preparation, Biogeosciences Discuss., 2012.

Bligh, E. G. and Dyer, W. J.: A rapid method of total lipid extraction and purification, Can. J. Biochem. Phys., 37, 911–917, 1959.

Brussaard, C. P. D.: Viral Control of Phytoplankton Populations – a Review, J. Eukaryot. Microbiol., 51, 125–138, 2004.

Brussaard, C. P. D., Noordeloos, A. A. M., Witte H., Collenteur, M. Schulz, K., Ludwig, A., Czerny, J., and Riebesell, U.: Arctic microbial community dynamics influenced by elevated CO_2 levels, in preparation, Biogeosciences Discuss., 2012.

Buesseler, K. O., Antia, A. N., Chen, M., Fowler, S. W., Gardner, W. D., Gustafsson, O., Harada, K., Michaels, A. F., van der Loeff'o, M. R., Sarin, M., Steinberg, D. K., and Trull, T.: An assessment of the use of sediment traps for estimating upper ocean particle fluxes, J. Mar. Res., 65, 345–416, 2007.

Burkhardt, S., Zondervan, I., and Riebesell, U.: Effect of CO_2 concentration on C : N : P ratio in marine phytoplankton: A species comparison, Limnol. Oceanogr., 44, 683–690, 1999.

Cole, J. J., Findlay, S., and Pace, M. L.: Bacterial production in fresh and saltwater ecosystems – a cross-system overview, Mar. Ecol.-Prog. Ser., 43, 1–10, 1988.

BGD
9, 8571–8610, 2012

Cranwell, P. A., Creighton, M. E., and Jaworski, G. H. M.: Lipids of four species of freshwater chrysophytes, Phytochemistry, 27, 1053–1059, doi:10.1016/0031-9422(88)80272-3, 1988.
Czerny, J., Bellerby, R. G. J., Boxhammer, T., Engel, A., Krug, S. A., Ludwig, A., Nachtigall, K., Niehoff, B. Schulz, K. G., and Riebesell, U.: Element budgets in an Arctic mesocosm CO_2 perturbation study, in preparation, Biogeosciences Discuss., 2012.
Czerny, J., Schulz, K. G., and Riebesell, U.: A simple method for gas exchange measurements in mesocosms and its application in mesocosm carbon budget calculations, in preparation, Biogeosciences Discuss., 2012.
de Kluijver, A., Soetaert, K., Schulz, K. G., Riebesell, U., Bellerby, R. G. J., and Middelburg, J. J.: Phytoplankton-bacteria coupling under elevated CO_2 levels: a stable isotope labelling study, Biogeosciences, 7, 3783–3797, doi:10.5194/bg-7-3783-2010, 2010.
del Giorgio, P. A. and Cole, J. J.: Bacterial growth efficiency in natural aquatic systems, Annu. Rev. Ecol. Syst., 29, 503–541, 1998.
Delille, B., Harlay, J., Zondervan, I., Jacquet, S., Chou, L., Wollast, R., Bellerby, R. G. J., Frankignoulle, M., Borges, A. V., Riebesell, U., and Gattuso, J. P.: Response of primary production and calcification to changes of pCO_2 during experimental blooms of the coccolithophorid Emiliania huxleyi, Glob. Biogeochem. Cycle, 19, 14, GB2023 doi:10.1029/2004gb002318, 2005.
Dijkman, N. A. and Kromkamp, J. C.: Phospholipid-derived fatty acids as chemotaxonomic markers for phytoplankton: application for inferring phytoplankton composition, Mar. Ecol.-Prog. Ser., 324, 113–125, 2006.
Dijkman, N. A., Boschker, H. T. S., Middelburg, J. J., and Kromkamp, J. C.: Group-specific primary production based on stable-isotope labeling of phospholipid-derived fatty acids, Limnol. Oceanogr.: Methods, 7, 612–625, 2009.
Engel, A.: Direct relationship between CO_2 uptake and transparent exopolymer particles production in natural phytoplankton, J. Plankton Res., 24, 49–53, 2002.
Engel, A., Thoms, S., Riebesell, U., Rochelle-Newall, E., and Zondervan, I.: Polysaccharide aggregation as a potential sink of marine dissolved organic carbon, Nature, 428, 929–932, 2004a.
Engel, A., Delille, B., Jacquet, S., Riebesell, U., Rochelle-Newall, E., Terbruggen, A., and Zondervan, I.: Transparent exopolymer particles and dissolved organic carbon production by Emiliania huxleyi exposed to different CO_2 concentrations: a mesocosm experiment, Aquat. Microb. Ecol., 34, 93–104, 2004b.

BGD
9, 8571–8610, 2012

Engel, A., Borchard, C., Piontek, J., Schulz, K. G., Bellerby, R. G. J.: CO_2 increases ^{14}C-primary production in an Arctic plankton community, in preparation, Biogeosciences Discuss., 2012.
Fry, B. (Ed.): Stable isotope ecology, Springer Science and Business Media, 2006.
Gelman, A.: Inference and monitoring convergence, Markov Chain Monte Carlo in Practice, 131–143, 1996.
Grossart, H. P., Allgaier, M., Passow, U., and Riebesell, U.: Testing the effect of CO_2 concentration on the dynamics of marine heterotrophic bacterioplankton, Limnol. Oceanogr., 51, 1–11, 2006.
Kaufman, M., Gradinger, R., Bluhm, B., and O'Brien, D.: Using stable isotopes to assess carbon and nitrogen turnover in the Arctic sympagic amphipod Onisimus litoralis, Oecologia, 158, 11–22, doi:10.1007/s00442-008-1122-y, 2008.
Kirchman, D. L., Moran, X. A. G., and Ducklow, H.: Microbial growth in the polar oceans – role of temperature and potential impact of climate change, Nat. Rev. Micro., 7, 451–459, 2009a.
Kirchman, D. L., Hill, V., Cottrell, M. T., Gradinger, R., Malmstrom, R. R., and Parker, A.: Standing stocks, production, and respiration of phytoplankton and heterotrophic bacteria in the Western Arctic Ocean, Deep Sea Research Pt. II, 56, 1237–1248, 2009b.
Leu, E., Daase, M., Schulz, K. G., Stuhr, A., and Riebesell, U.: Effect of ocean acidification on the fatty acid composition of a natural plankton community, Biogeosciences Discuss., 9, 8173–8197, doi:10.5194/bgd-9-8173-2012, 2012.
Legendre, L. and Rassoulzadegan, F.: Plankton and nutrient dynamics in marine waters, Ophelia, 41, 153–172, 1995.
Middelburg, J. J., Barranguet, C., Boschker, H. T. S., Herman, P. M. J., Moens, T., and Heip, C. H. R.: The fate of intertidal microphytobenthos carbon: An in situ ^{13}C-labeling study, Limnol. Oceanogr., 45, 1224–1234, 2000.
Niehoff, B., Knüppel, N., Daase, M., Czerny, J., and Boxhammer, T.: Mesozooplankton community development at elevated CO_2 concentrations: Results from a mesocosm experiment in a high Arctic fjord, in preparation, Biogeosciences Discuss., 2012.
Osburn, C. L. and St-Jean, G.: The use of wet chemical oxidation with high-amplification isotope ratio mass spectrometry (WCO-IRMS) to measure stable isotope values of dissolved organic carbon in seawater, Limnol. Oceanogr. Meth., 5, 296–308, 2007.
Peduzzi, P. and Weinbauer, M. G.: Effect of concentrating the virus-rich 2–200 nm size fraction of seawater on the formation of algal flocs (Marine Snow), Limnol. Oceanogr., 38, 1562–1565, 1993.

BGD
9, 8571–8610, 2012

Piontek, J., Borchard, C., Sperling, M., Schulz, K. G., Riebesell, U., and Engel, A.: Response of bacterioplankton activity in an Arctic fjord system to elevated pCO_2: results from a mesocosm perturbation study, in preparation, Biogeosciences Discuss., 2012.

Riebesell, U., Schulz, K. G., Bellerby, R. G. J., Botros, M., Fritsche, P., Meyerhofer, M., Neill, C., Nondal, G., Oschlies, A., Wohlers, J., and Zollner, E.: Enhanced biological carbon consumption in a high CO_2 ocean, Nature, 450, 545–549, 2007.

Riebesell, U., Kortzinger, A., and Oschlies, A.: Sensitivities of marine carbon fluxes to ocean change, Proc. Natl. Acad. Sci. USA, 106, 20602–20609, doi:10.1073/pnas.0813291106, 2009.

Rivkin, R. B. and Legendre, L.: Biogenic carbon cycling in the upper ocean: effects of microbial respiration, Science, 291, 2398–2400, 2001.

Rokkan Iversen, K. and Seuthe, L.: Seasonal microbial processes in a high-latitude fjord (Kongsfjorden, Svalbard): I. heterotrophic bacteria, picoplankton and nanoflagellates, Polar Biol., 1–19, 2010.

Schulz, K. G., Riebesell, U., Bellerby, R. G. J., Biswas, H., Meyerhöfer, M., Müller, M. N., Egge, J. K., Nejstgaard, J. C., Neill, C., Wohlers, J., and Zöllner, E.: Build-up and decline of organic matter during PeECE III, Biogeosciences, 5, 707–718, doi:10.5194/bg-5-707-2008, 2008.

Schulz, K. G., Bellerby, R. G. J., Brussaard, C. P. D., Büdenbender, J., Czerny, J., Fischer, M., Koch-Klavsen, S., Krug, S. A., Lischka, S., Ludwig, A., Meyerhöfer, M., Nondal, G., Silyakova, A., Stuhr, A., and Riebsull U.: Temporal biomass dynamics of an Arctic plankton bloom in response to increasing levels of atmospheric carbon dioxide, in preparation, Biogeosciences Discuss., 2012.

Soetaert, K. and Petzoldt, T.: FME: A Flexible Modelling Environment for inverse modelling, sensitivity, identifiability, monte carlo analysis, R package version, 1, 2009.

Soetaert, K., Petzoldt, T., and Setzer, R. W.: deSolve: General solvers for initial value problems of ordinary differential equations (ODE), partial differential equations (PDE) and differential algebraic equations (DAE), R package version, 1, 2009.

Steinacher, M., Joos, F., Frölicher, T. L., Plattner, G.-K., and Doney, S. C.: Imminent ocean acidification in the Arctic projected with the NCAR global coupled carbon cycle-climate model, Biogeosciences, 6, 515–533, doi:10.5194/bg-6-515-2009, 2009.

Tanaka, T., Alliouane, S., Bellerby, R. G. J., Czerny, J., de Kluijver, A., Engel, A., Schulz, K. G., Silyakova, A., and Gattuso J- P.: Metabolic balance of a plankton community in Arctic coastal waters in response to increased pCO_2, in preparation, Biogeosciences Discuss., 2012.

BGD
9, 8571–8610, 2012

Thingstad, T., Bellerby, R., Bratbak, G., Børsheim, K., Egge, J., Heldal, M., Larsen, A., Neill, C., Nejstgaard, J., and Norland, S.: Counterintuitive carbon-to-nutrient coupling in an Arctic pelagic ecosystem, Nature, 455, 387–390, 2008.

Van den Meersche, K., Middelburg, J. J., Soetaert, K., van Rijswijk, P., Boschker, H. T. S., and Heip, C. H. R.: Carbon-nitrogen coupling and algal-bacterial interactions during an experimental bloom: Modeling a ^{13}C tracer experiment, Limnol. Oceanogr., 49, 862–878, 2004.

Van den Meersche, K., Soetaert, K., and Middelburg, J. J.: Plankton dynamics in an estuarine plume: a mesocosm ^{13}C and ^{15}N tracer study, Mar. Ecol.-Prog. Ser., 429, 29–43, doi:10.3354/meps09097, 2011.

Van Engeland, T., De Kluijver, A., Soetaert, K., Meysman, F., and Middelburg, J. J.: Isotope information improves predictive capabilities of a biogeochemical model, in preparation, Biogeosciences Discuss., 2012.

Zhang, J., Quay, P. D., and Wilbur, D. O.: Carbon-isotope fractionation during gas-water exchange and dissolution of CO_2, Geochim. Cosmochim. Acta, 59, 107–114, 1995.

BGD

9, 8571–8610, 2012

Table 1. Growth (μ) and production (P) rates based on Eqs. (1) and (3), respectively, for each phase. Values are presented as average of all mesocosms ± standard deviation (n = 9).

	Growth rate (μ, days^{-1})			Production rate (P, µmol C l^{-1} days^{-1})		
	Phase 1 (t_{0-6})	Phase 1 (t_{0-12})	Phase 2 (t_{14-29})	Phase 1 (t_{0-6})	Phase 1 (t_{0-12})	Phase 2 (t_{14-29})
Phyto I	0.85 ± 0.06	0.19 ± 0.08	–	0.65 ± 0.08	0.19 ± 0.08	
Phyto II	0.48 ± 0.04	0.23 ± 0.02	0.22 ± 0.06	0.55 ± 0.06	0.30 ± 0.06	0.40 ± 0.13
Bac	0.68 ± 0.11	0.33 ± 0.02	0.13 ± 0.04		0.47 ± 0.03	0.20 ± 0.15
POC					0.80 ± 0.13	0.75 ± 0.22

BGD
9, 8571–8610, 2012

Table 2. Parameter descriptions and values of the food web model for phase 1 (t_{0-12}). Values are presented as average of all mesocosms ± standard deviation ($n = 9$) derived from MCMC fitting procedures.

Parameters that were tested for different CO_2 levels			
Parameter	Unit	Description	Value
μ_{I}	$days^{-1}$	growth rate of Phyto I	0.87 ± 0.013
μ_{II}	$days^{-1}$	growth rate of Phyto II	0.18 ± 0.010
ξ_{I}	$days^{-1}$	mortality rate of Phyto I	0.29 ± 0.081
ξ_{II}	$days^{-1}$	mortality rate of Phyto II	0.045 ± 0.025
μ_{g}	$days^{-1}$	grazing rate of Zooplankton	0.022 ± 0.005
γ_{I}	$days^{-1}$	exudation rate of Phyto I	0.31 ± 0.023
γ_{II}	$days^{-1}$	exudation rate of Phyto II	0.24 ± 0.017
μ_{Bac}	$days^{-1}$	growth rate of Bacteria	0.36 ± 0.029
r_{sink}	$days^{-1}$	sinking rate of detritus	0.0082 ± 0.0048
ρ	$days^{-1}$	mineralisation rate	0.020 ± 0.004
f_{DOM}	–	part of Phyto mortality to DOM	0.056 ± 0.037
f_{Det}	–	part of Phyto mortality to detritus	0.37 ± 0.05
Parameters that were kept constant for different CO_2 levels			
Parameter	Unit	Description	Value
ε_{N}	$\mu mol\,l^{-1}$	half saturation constant for DIN	0.5
ε_{I}	$W\,m^{-2}$	half saturation constant for light	120
ε_{g}	$\mu mol\,l^{-1}$	half saturation constant for phyto I + II	1
ε_{DOC}	$\mu mol\,l^{-1}$	half saturation constant for LDOC	0.001
f_{faeces}	–	part of zooplankton grazing to faeces	0.149
ξ_{Zoo}	–	part of zooplankton swimming into traps	0.654
NC	–	stoichiometric ratio	16/106

BGD
9, 8571–8610, 2012

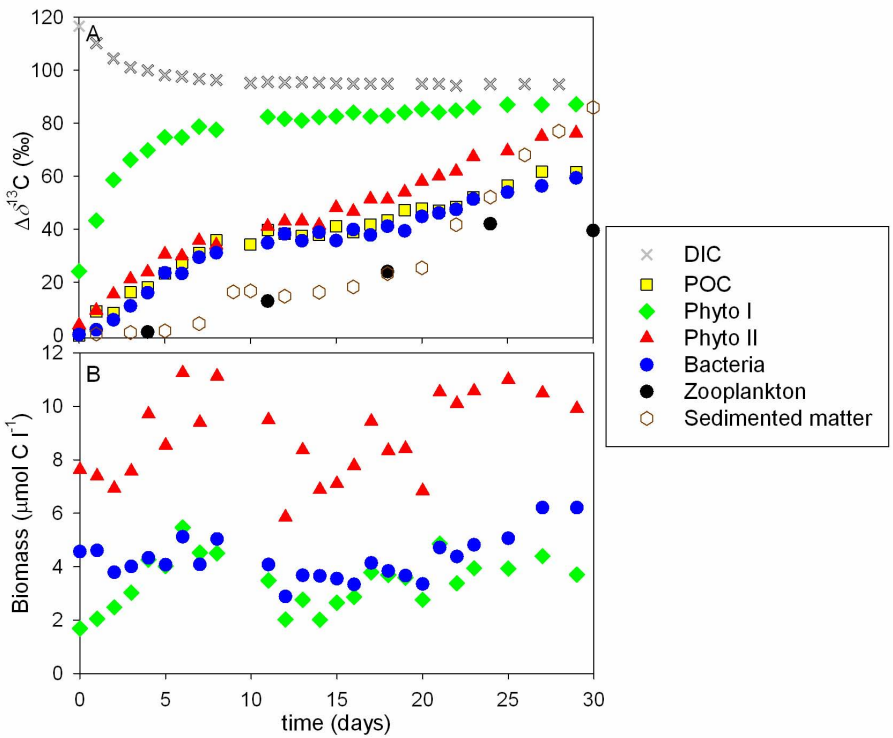

Fig. 1. The temporal change as averaged over all mesocosms ($n = 9$) of **(A)** isotope ratios ($\Delta\delta^{13}C$) of all measured carbon pools, and **(B)** of biomass (µmol C l^{-1}) of phyto I, phyto II, and bacteria.

BGD
9, 8571–8610, 2012

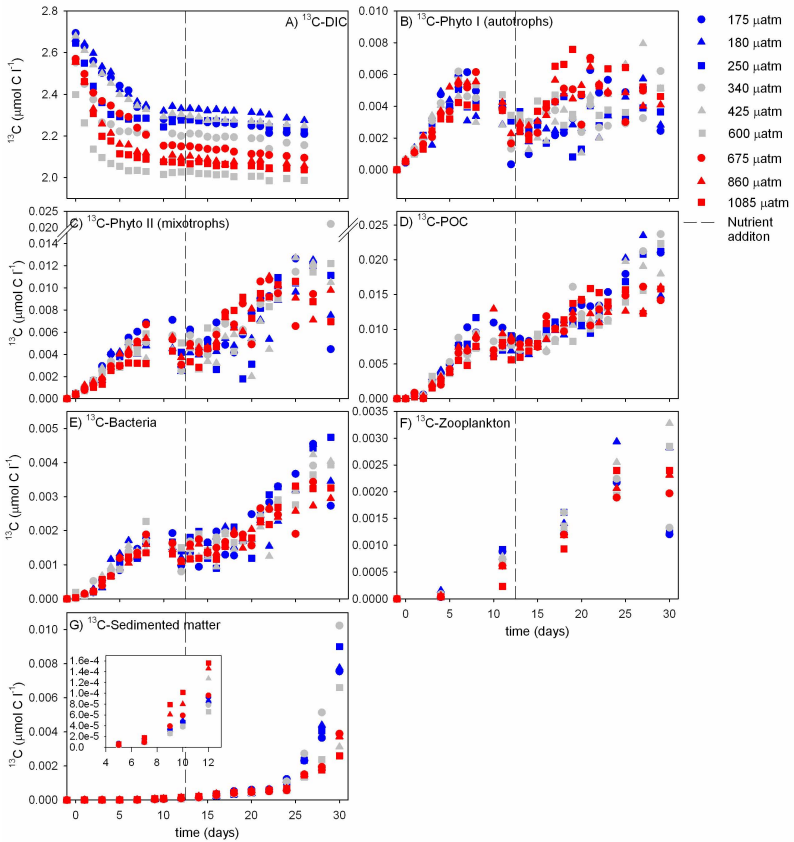

Fig. 2. Temporal development of ^{13}C in stocks and ^{13}C labelled biomass (µmol ^{13}C l^{-1}) of **(A)** DIC; **(B)** Phyto I; **(C)** Phyto II; **(D)** POC; **(E)** Bacteria; **(F)** Zooplankton (*Calanus* sp.); and **(G)** Sedimented organic matter in each mesocosm. Red colours are used for high pCO_2 treatments, grey for medium, and blue for low pCO_2 treatments. The vertical line denotes the timing of nutrient addition. The inset of **(G)** zooms in on the first phase.

BGD
9, 8571–8610, 2012

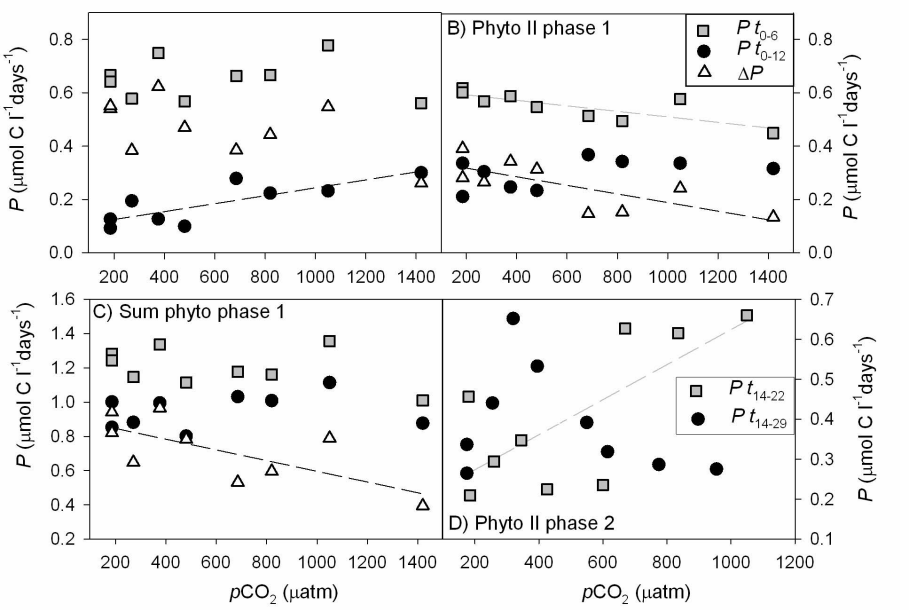

Fig. 3. Production rates vs. average pCO_2 levels of each phase based on data (Eq. 3) of **(A)** Phyto I; **(B)** Phyto II; and **(C)** sum phyto I and II production rates ($\mu mol\,C\,l^{-1}\,days^{-1}$) in phase 1 for the build-up ($t_{0–6}$), the build-up and decline ($t_{0–12}$), and the production loss during decline (difference) denoted with Δ; **(D)** Phyto II production rates ($\mu mol\,C\,l^{-1}\,days^{-1}$) after nutrient addition for initial phase 2 ($t_{14–22}$) and total phase 2 ($t_{14–29}$).

BGD
9, 8571–8610, 2012

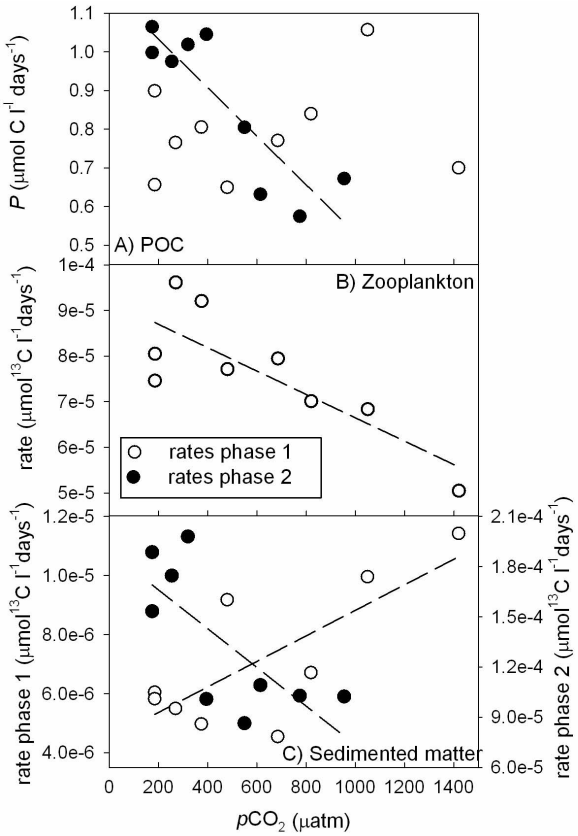

Fig. 4. (A) POC production ($\mu mol\,C\,l^{-1}\,days^{-1}$) before (phase 1) and after nutrient addition (phase 2); **(B)** ^{13}C increase in zooplankton ($\mu mol\,^{13}C\,l^{-1}\,days^{-1}$) from t_{0-18}); **(C)** ^{13}C increase in cumulative sedimented organic matter ($\mu mol\,^{13}C\,l^{-1}\,days^{-1}$) before (phase 1) and after nutrient addition (phase 2) as function of average pCO_2 levels of the corresponding phase.

BGD
9, 8571–8610, 2012

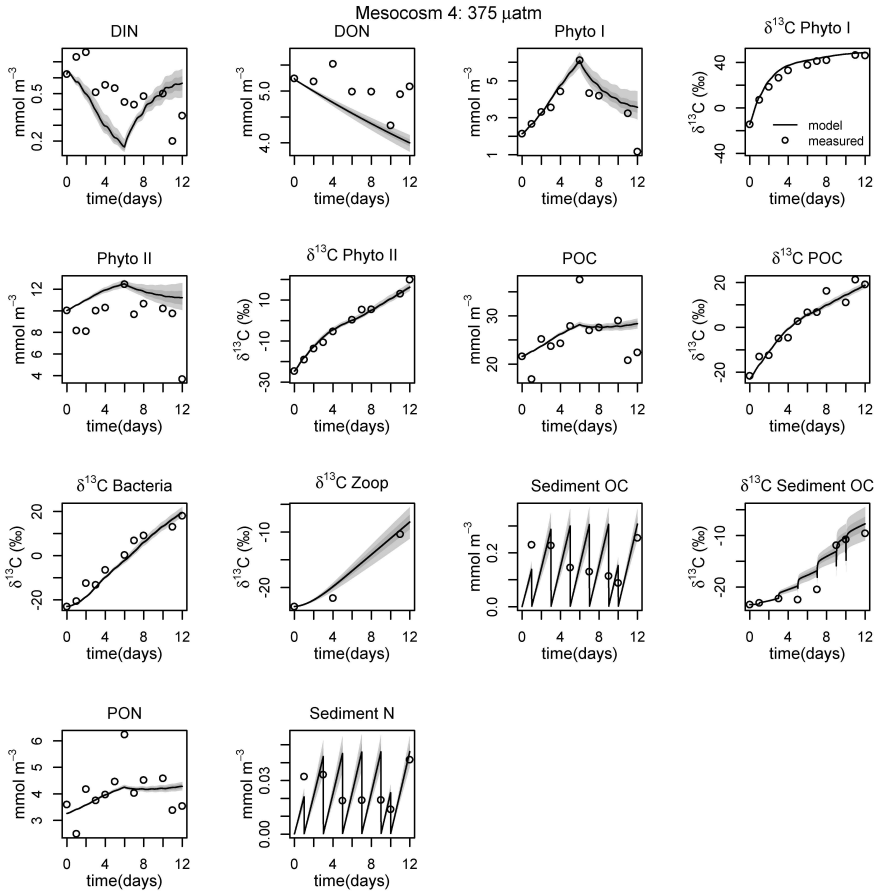

Fig. 5. MCMC plots showing the best fits of model output (solid line) with uncertainty (grey envelopes) fitted to the data (points) for one mesocosm (M4, 375 µatm). Fits of the other mesocosms are presented in the supplementary material.

BGD
9, 8571–8610, 2012

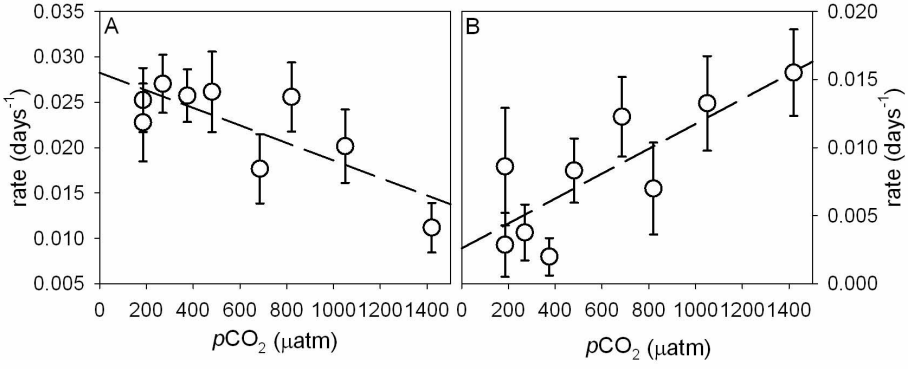

Fig. 6. Model parameters (days^{-1}) with uncertainties for **(A)** zooplankton grazing rates (μ_g) and **(B)** sinking rates (r_{sink}) vs. average pCO$_2$ levels in phase 1.

BGD
9, 8571–8610, 2012

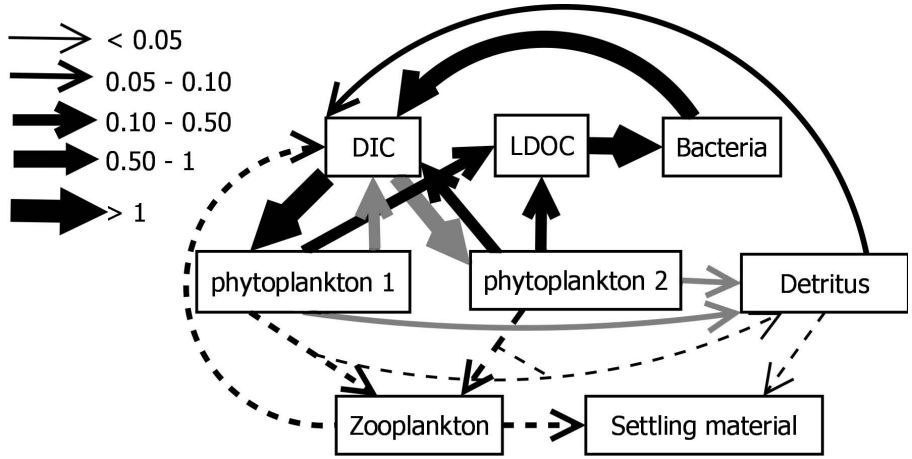

Fig. 7. Model-based carbon flow chart of phase 1 (before nutrient addition). The thicknesses of the arrows represent the size of the average carbon fluxes ($\mu mol\,C\,l^{-1}\,days^{-1}$) between the major carbon pools. The dashed arrows indicate fluxes that were CO_2 sensitive (based on model). The grey arrows indicate fluxes that may depend on pCO_2 based on data analyses (Fig. 3).

BGD
9, 8571–8610, 2012